31st Annual International Conference of the IEEE EMBS
Minneapolis, Minnesota, USA, September 2-6, 2009

Iterative Image Reconstruction Model Including Susceptibility Gradients Combined with Z-shimming Gradients in fMRI

Yue Zhuo, *Student Member, IEEE*, and Bradley P. Sutton, *Member, IEEE*
Bioengineering Department, University of Illinois at Urbana-Champaign

***Abstract*—Magnetic susceptibility artifacts, including both image distortions and signal losses, exist near air/tissue interfaces in the ventral brain in standard blood oxygenation level dependent (BOLD) functional magnetic resonance imaging (fMRI). Although several acquisition-based approaches exist to address the signal losses, they require increased acquisition time or patient customization. In this work, we propose a statistical estimation model that includes the effects of magnetic field gradients (both within-plane and through-plane gradients) and uses an iterative reconstruction algorithm to reconstruct images corrected for both magnetic field distortion and signal losses. Besides, we combine our reconstruction approach with a recently proposed MRI sequence with Z-shimming gradient between the spiral-in and spiral-out acquisition to enhance the compensation for signal losses. Therefore, we extend our forward MR signal model to include the physics of Susceptibility-induced magnetic Field (SF), Susceptibility-induced magnetic Field Gradients (SFG), and the application of the data acquisition technique with Z-shimming Gradients (ZShG). The results show that not only signal distortions but also significant signal losses can be compensated by considering both the modeling of field-inhomogeneity effects along with the acquisition using Z-shimming.**

I. INTRODUCTION

FOR functional magnetic resonance imaging (fMRI) with blood oxygenation level-dependent (BOLD) contrast, the long readout times make the functional scan sensitive to magnetic inhomogeneity. Without compensation, the susceptibility differences near air/tissue interfaces, especially at the ventral brain (e.g. above the sphenoid and frontal sinuses), will induce field inhomogeneity which leads to susceptibility artifacts including image geometric distortions and signal losses.

Several methods exist for compensating the susceptibility-induced magnetic field inhomogeneity (SF) [1-10]. Non-iterative, Fourier-based correction methods (e.g. Conjugate Phase [8], etc.) can compensate for image distortion artifacts, but susceptibility-induced signal losses are not addressed by these methods. Signal losses result from susceptibility-induced magnetic field gradients (SFG), which cause spin dephasing within a voxel [9-15]. Although several acquisition-based approaches (e.g. hardware-Shim, tailored RF pulses, thinner slices, etc.) exist to address the signal losses, they require increased acquisition time or have to be tailored to patient specific field map. A natural alternative is to build a statistical estimation model and use iterative algorithm to perform reconstruction while modeling the susceptibility gradients that lead to signal losses. Previous work builds a physical model that accounts for both within-plane gradients and through-plane gradients of the field inhomogeneity to correct for geometric distortions and signal losses [13-16].

When the susceptibility gradients are too large, the signal losses will be too severe so that the signals will be too weak to be extracted from the noise. In this case, we might benefit from additional information gathered during data acquisition. The Z-shimming gradients (ZShG) technique in data acquisition has been used to reduce susceptibility artifacts [17], but with a cost of increased scan time. The scan must be repeated for each value of Z-shimming. A recently proposed method includes Z-shimming in a single-shot spiral scan trajectory, combines spiral-in and spiral-out with a single Z-shim step in between. The single shot Z-shimming method decreases the acquisition time considerably [18]. However, combination of the images from each part of the acquisition requires choosing a weighting scheme.

In this work, we introduce an iterative, inverse approach to reconstruct the fMRI image compensating for the susceptibility artifacts based on building a model that includes the field map, its linear susceptibility gradients, and the application of the acquisition technique with Z-shimming.

II. THEORY

In this section, we will describe the proposed signal model which is including the field map and its linear susceptibility gradients, and Z-shimming gradients. Then we will explain the piecewise linear model of the basis expansion for magnetic field inhomogeneity. Finally the iterative algorithm using the proposed imaging model will be presented for the fMRI image reconstruction

A. Signal Model

In MRI scan, the measurements of raw data are noisy samples of the signal as shown in equation (1):

$$y_m = S(t_m) + \varepsilon_m, \qquad m = 1,...,M \ , \tag{1}$$

where $S(t_m)$ is the complex MR signal at time t_m during the readout; ε_m is the complex white Gaussian noise at time t_m which is introduced during the data acquisition; M is the number of k-space samples.

In this paper, we use a 2D spiral protocol for MR image acquisition. For a 2D data acquisition in each slice, the signal $s(t_m)$ at each t_m can be written as

$$S(k_x(t_m),k_y(t_m),k_z(t_m)) = \int_{z_0-\frac{\Delta z}{2}}^{z_0+\frac{\Delta z}{2}} \int \int_{-\frac{FOV}{2}}^{\frac{FOV}{2}} f(x,y,z) e^{-i2\pi\omega(x,y,z)t_m} \cdot e^{-i2\pi[k_x(t_m)x+k_y(t_m)y+k_z(t_m)z]} dxdydz, \quad (2)$$

where z_0 is the slice location in through-plane direction for each slice, and Δ_z is the slice thickness; FOV is the field of view for 2D spiral acquisition; $f(x,y,z)$ is a function of the object's transverse magnetization at location (x,y,z) in the selected slice; $\omega(x,y,z)$ is the field inhomogeneity map (in Hz) including both the within-plane gradient ([X, Y] or [read, phase] directions) and through-plane gradient (Z or slice direction), which can be determined by a pre-scan [14, 16]; $k_x(t_m)$ and $k_y(t_m)$ is the k-space trajectory along X and Y directions, and $k_z(t_m)$ represents the application of Z-shimming.

B. Basis Expansion

Our MR imaging reconstruction challenge is to estimate the object $f(x,y,z)$ that closely matches the measurements of raw data y_m (m=1,..,M). From equation (2), we know that this is an ill-posed problem, because $f(x,y,z)$ is a continuous function but the measurements vector $\boldsymbol{Y}$=[y_1, ...,y_M] is discrete since we only have finite samples. We proceed by parameterizing the object $f(x,y,z)$ and field inhomogeneity map $\omega(x,y,z)$ in terms of basis functions $\varphi_n(x,y,z)$ as follows

$$f(x,y,z) \approx \sum_{n=0}^{N-1} f_n \varphi_n(x,y,z), \quad (3)$$

$$\omega(x,y,z) \approx \sum_{n=0}^{N-1} \left(\omega_n + \mathrm{G}_{Xn}(x-x_n) + \mathrm{G}_{Yn}(y-y_n) + \mathrm{G}_{Zn}(z-z_0)\right) \cdot \varphi_n(x,y,z) \quad (4)$$

where for each slice, (x_n, y_n) is the in-plane center of every voxel; ω_n is the off-resonance frequency for each voxel (in Hz); G_{Xn}, G_{Yn} are the within-plane gradients (in Hz/m) and G_{Zn} is the through-plane gradient within each voxel (in Hz/m); N is the number of voxels. Here we use 3D rectangle functions as the basis function

$$\varphi_n(x,y,z) = rect_3\left(\frac{x-x_n}{\Delta_x}, \frac{y-y_n}{\Delta_y}, \frac{z-z_0}{\Delta_z}\right), \quad (5)$$

where Δ_x, Δ_y are the in-plane dimensions of each voxel. Substituting Eq. (3)-(5) into the signal model in Eq. (2) and simplifying yields

$$S(k_x(t_m),k_y(t_m),k_z(t_m)) = \sum_{n=0}^{N-1} f_n e^{-i2\pi\omega_n t_m} e^{-i2\pi[k_x(t_m)x_n+k_y(t_m)y_n]} \cdot \Phi_n(k_x(t_m),k_y(t_m),k_z(t_m)) e^{-i2\pi k_z(t_m)z_0}, \quad (6)$$

where $\Phi_n(k_x(t_m), k_y(t_m), k_z(t_m))$ is the Fourier Transform of the basis function of $\varphi_n(x,y,z)$ combined with the effects of the gradients of field inhomogeneity, which can be written as

$$\Phi_n(k_x(t_m),k_y(t_m),k_z(t_m)) = sinc\left(\left(k_x(t_m)+G_{Xn}t_m\right)\Delta_x\right) \cdot sinc\left(\left(k_y(t_m)+G_{Yn}t_m\right)\Delta_y\right) sinc\left(\left(k_z(t_m)+G_{Zn}t_m\right)\Delta_z\right). \quad (7)$$

In our case, the effect of through-plane gradient G_{Zn} and the effect of Z-shimming gradient $k_z(t_m)$ are both modeled inside the third $sinc(\cdot)$ term. If term $k_z(t_m)$ for Z-shimming gradient effect is equal to zero, then the proposed model is equivalent to one of our previous approach described in [14, 16].

C. Iterative Algorithms

We can express the measured noisy samples in Eq. (1) in matrix-vector form:

$$\mathbf{y} = \mathbf{S} + \boldsymbol{\varepsilon} = \mathbf{A}\mathbf{f} + \boldsymbol{\varepsilon}, \quad (8)$$

where $\mathbf{y}$ is the measured noisy data samples at the k-space locations arranged as a single column vector; $\mathbf{S}$ is the signal modeled as above; $\mathbf{f}$ is the object also as a single column vector; $\boldsymbol{\varepsilon}$ is the complex white Gaussian noise; $\mathbf{A}$ is the system matrix with dimension M×N, which denotes the data acquisition procedure, with the elements a_{mn} shown as follows

$$a_{mn} = \Phi_n(k_x(t_m),k_y(t_m),k_z(t_m)) e^{-i2\pi k_z(t_m)z_0} e^{-i2\pi\omega_n t_m} \cdot e^{-i2\pi[k_x(t_m)x_n+k_y(t_m)y_n]}. \quad (9)$$

Here, since we use two acquisitions (spiral-in and spiral-out with Z-shimming in between), our system matrix $\mathbf{A}$ is a stacked version, i.e. the system matrix $\mathbf{A_{in}}$ for an individual spiral-in acquisition (that includes SF map (SFM) and SFG map (SFGM), but without Z-shimming) is stacked on the top of a system matrix $\mathbf{A_{out}}$ for a spiral-out acquisition (with SFM, SFGM and Z-shimming explicitly modeled). The magnetic susceptibility (in both $\mathbf{A_{in}}$ and $\mathbf{A_{out}}$) is in the term $exp(-i\omega_n t_m)$, while the magnetic susceptibility gradients (in both $\mathbf{A_{in}}$ and $\mathbf{A_{out}}$) and Z-shimming gradient (in $\mathbf{A_{out}}$ only) are both modeled inside the term $\Phi_n(k_x(t_m), k_y(t_m), k_z(t_m))$ as described in Eq. (7).

The object $\mathbf{f}$ is estimated by minimizing a quadratic penalized least-square cost function $\Psi(\mathbf{f})$,

$$\hat{\mathbf{f}} = \arg\min_{\mathbf{f}} \boldsymbol{\Psi}(\mathbf{f}),$$

$$\boldsymbol{\Psi}(\mathbf{f}) = \frac{1}{2}\left\|\mathbf{y}-\mathbf{A}\mathbf{f}\right\|_2^2 + \beta R(\mathbf{f}), \quad (10)$$

where $\|\cdot\|_2$ is the 2-norm of a matrix (square root of sum of square of all the elements); β is the regulation parameter chosen so it has little impact on the spatial resolution of the reconstruction; and $R(\mathbf{f})$ is a regularization function, which penalizes the roughness of the estimated image to control noise, as defined

$$R(\mathbf{f}) = \frac{1}{2}\left\|\mathbf{C}\mathbf{f}\right\|_2^2, \quad (11)$$

where the matrix $\mathbf{C}$ takes differences between in-plane neighboring voxels [19]. This regularization function $R(\mathbf{f})$ can decrease the condition number of the image reconstruction. We apply the iterative algorithm of conjugate gradients (CG) for minimizing the cost function $\Psi(\mathbf{f})$ [19].

III. Methods and Results

To evaluate the proposed methods, we performed simulation, phantom and in vivo studies. Currently another

commonly used method for susceptibility artifacts compensation is non-iterative reconstruction using SFM (conjugate phase reconstruction [2]) combined with Z-shimming. Therefore, we compared the results of this non-iterative method (Method 1: NIT+SFM+ZShG, non-iterative method including sum-of-squares combination of spiral-in and spiral-out acquisition data), with our proposed iterative method (Method 2: IT+SFM+SFGM+ZShG, iterative algorithm including the field map, its linear susceptibility gradients, and Z-shimming in the reconstruction model).

A. Simulation study

The goal of the simulation study is to examine the efficiency of the proposed methods for compensation of susceptibility artifacts induced by the field inhomogeneity. The noisy simulation data **y** were formed by constructing a high-resolution model of the human brain at a matrix size of 256×256 and then applying Eq. (2) to compute the signal **S** at the desired k-space locations for sampling a 64×64 image and adding white Gaussian noise **ε**. Images were then reconstructed from the simulation data using Methods 1 and 2.

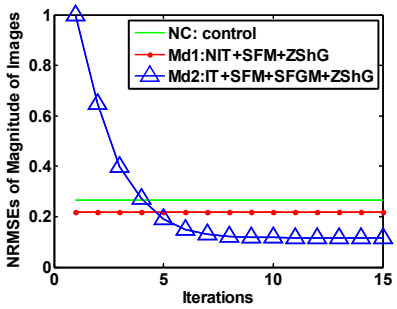

Fig. 1. Evaluation of Simulation Result: Comparison of the NRMSEs for the resulting image from non-iterative method (Method 1: NIT + SFM + ZShG) and the resulting image from our iterative method (Method 2: IT + SFM + SFGM + ZShG) along with iterations R_n. Where the green solid line shows the non-compensated image (NC) as control; the red line with point marks shows the $NRMSE_1$ between reference image and the Method 1; the blue line with triangle marks shows the $NRMSE_2$ between the reference image and out proposed Method 2.

To evaluate the quality of resulting image and efficiency for the proposed method, we calculated the normalized root-mean-squared errors (NRMSEs) in the region of interest (ROI) as follows

$$NRMSE = \frac{\left\| \mathbf{f}_0 - \hat{\mathbf{f}}_c \right\|_2}{\left\| \mathbf{f}_0 \right\|_2}, \qquad (12)$$

where $\mathbf{f}_0$ is the reference image downsampled to 64×64; $\hat{\mathbf{f}}_c$ is the results of estimated images compensated with either of two methods. We compared the $NRMSE_1$ between reference image and result from the non-iterative method (Method 1) on one side and the $NRMSE_2$ between reference image and result from the proposed iterative method (Method 2) along with various numbers of iteration. We also used non-compensated image (NC) for comparison (shown in Fig. 1).

As shown in Fig. 1, we examined the first 15 iterations of the NRMSEs for our iterative method. The proposed method (Method 2) converges fast in the first several iterations, and already has lower errors after iteration 5 compared with the non-iterative method (Method 1).

B. Phantom and in vivo study

For the phantom and in vivo study, the experiments were performed on a head-only Siemens Allegra 3T MRI scanner. The data scan parameters are given as follows: matrix size 64×64, field of view (FOV) 0.24 m, slice thickness 4×10^{-3} m, TR 2 s, TE 35 ms, number of slices 20.

The field map was acquired using a pre-scan of multi-echo gradient echo sequence with similar slice prescription, but twice the resolution in all directions for estimating the susceptibility gradients map in Z-direction[14], with TR 200 ms, and TE 10 and 12.46 ms. In the functional scanning, we use a spiral-in-and-out trajectory with Z-shimming in between, as described in [18]. The spiral-in trajectory, which starts k-space sampling from the peripheral region and ends at the center is followed by the Z-shimming gradient (4 mT/m for 1 ms), then is followed by the spiral-out acquisition. There is a 1.5 ms gap between the spiral-in and spiral-out acquisitions. In this way the spiral-in-and-out acquisition with Z-shimming would enhance the compensation for signal losses.

The phantom was made by 2% agar with water. In order to mimic the air/tissue interface which caused the magnetic field inhomogeneity in the ventral brain, we placed a ping-pong ball in the middle of the phantom. There are plastic grids around the ping-pong ball for physical support and also working as the tissue structure. We calculate the susceptibility-induced magnetic field map and its gradients in the phantom, as shown in Fig 2. It clearly shows that the field inhomogeneity exists in the air/agar interface inside the phantom, and its linear gradients in X, Y, Z directions (pointed by the red arrows) exist and can reach to ±1 Hz/m.

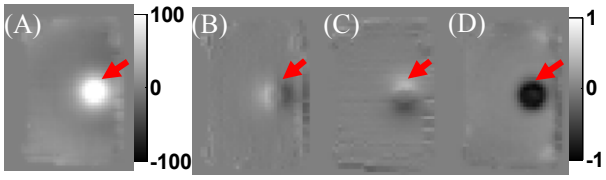

Fig. 2. Magnetic field inhomogeneity in the Phantom. (A) Field map (SFM) in Hz, (B-D) Susceptibility gradients (SFGM) in X, Y, Z directions in Hz/m, respectively.

The results obtained from phantom and in vivo data are shown in Fig 3 (A-D is phantom and E-H is in vivo). (A,E)

correspond to non-iterative reconstruction obtained with no compensation (NC); (B,F) show the effect of Z-shimming; (C,G) are the result for the non-iterative reconstruction with field map and Z-shimming (Method 1); and (D,H) are our proposed method which performs iterative reconstruction while including the field map (SFM), its linear susceptibility gradients (SFGM in X, Y, Z directions) and using the Z-shimming acquisition method (ZShG). The results for phantom study clearly show that our proposed iterative method (Method 2) with joint compensation of field map and its linear susceptibilities gradients, and Z-shimming significantly improves the image quality compared with non-iterative method.

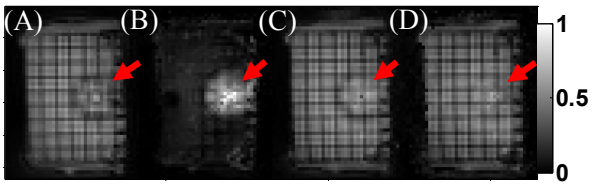

Fig.3. (A-D) Phantom study results

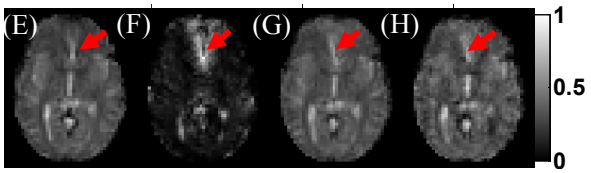

Fig.3. (E-H) In vivo study results

Fig. 3. For (A-D) Phantom study and (E-H) In vivo study, the image reconstruction rsults are: (A, E) Non compensation (NC), (B, F) Effect of ZShG, (C, G) NIT + SFM + ZShG (Method 1), (D, H) IT + SFM + SFMG + ZShG (Method 2).

We compared the results of non-iterative reconstruction (Method 1 (C, G)) with our proposed iterative algorithm (Method 2 (D, H)) as shown in Fig. 3. Preliminary results obtained in vivo from a volunteer subject are reported in Fig. 3 (E-H). As for the phantom results, increase in intensity in the degraded region is visible. Quantitative comparison analysis is showed in part A as simulation study. Further work will focus on improving the quality of the images for clinical data.

IV. Conclusion

In summary, the proposed method is an iterative image reconstruction method using the MRI image model which is including the physics of the susceptibility-induced magnetic field map (SFM), the gradients of field map (SFGM), and the Z-shimming gradients (ZShG) in data acquisition. The presented results show that the proposed method reduced the susceptibility artifacts of both signal distortion and significant signal losses, and image quality was significantly improved.

References

[1] K. Sekihara, M. Kuroda, H. Kohno. "Image restoration from non-uniform magnetic field influence for direct Fourier NMR imaging," *Phys Med Biol*, 1984. 29(1): p.15-24.

[2] D. C. Noll, C. H. Meyer, J. M. Pauly, D.G. Nishimura, A. Macovski, A homogeneity correction method for magnetic resonance imaging with time-varying gradients, *IEEE Trans Med Imaging*, 1991; 10 (4): p.629-37.

[3] P. Jezzard, R. S. Balaban. "Correction for geometric distortion in echo planar images from B0 field variations," *Magn Reson Med*, 1995. 34: p.65-73

[4] L. C. Man, J. M. Pauly, A. Macovski. Improved automatic off-resonance correction without a field map in spiral imaging. *Magn Reson Med*, 1997. 37: p.906-13.

[5] P. J. Reber, E. C. Wong, R. B. Buxton, L. R. Frank. "Correction of off resonance-related distortion in echo-planar imaging using EPI-based field maps," *Magn Reson Med*, 1998. 39: p.328-330.

[6] H. Schomberg, "Off-resonance correction of MR images," *IEEE Trans Med Imaging*, 1999.18(6): p. 481-495.

[7] R. Deichmann, O. Josephs, C. Hutton, D. R. Corfield, R. Turner. "Compensation of susceptibility-induced BOLD sensitivity losses in echo-planar fMRI imaging," *Neuroimage*. 2002 Jan. 15(1): p.120-35.

[8] D. C. Noll, J. A. Fessler, B. P. Sutton. "Conjugate phase MRI reconstruction with spatially variant sample density correction," *IEEE Trans Med Imaging*, 2005. 24(3): p.325-36.

[9] B. P. Sutton, D. C. Noll, and J. A. Fessler, Fast, iterative image reconstruction for MRI in the presence of field inhomogeneities, *IEEE Trans Med Imag*, 2003 Feb; vol. 22, no. 2, p.178–88.

[10] G. Liu, S. Ogawa, EPI image reconstruction with correction of distortion and signal losses. *J Magn Reson Imaging*, 2006 Sep; 24 (3): p.683-9.

[11] V. A. Stenger, F. E. Boada, D. C. Noll. "Multishot 3D slice-select tailored RF pulses for MRI," *Magn Reson Med*, 2002. 48(1): p.157-165.

[12] T. Q. Li, A. Takahashi, Y. Wang, V. Mathews, G. H. Glover. "Dual-echo spiral in/in acquisition method for reducing magnetic susceptibility artifacts in blood-oxygen-level-dependent functional magnetic resonance imaging," *Magn Reson Med,* 2006. 55(2): p.325-34.

[13] J. R. Reichenbach, R. Venkatesan, D. A. Yablonskiy, M. R. Thompson, S. Lai, E. M. Haacke. 1997. Theory and application of static field inhomogeneity effects in gradient echo imaging. *J Magn Reson Imaging*, 1997. 7(2): p.266-79.

[14] B. P. Sutton, D. C. Noll, and J. A. Fessler, Compensating for within voxel susceptibility gradients in BOLD fMRI, *Proc Int Soc Mag Res Med*, 2004; p.349.

[15] J. A. Fessler, D. C. Noll, Model-based MR Image Reconstruction with Compensation for Through-Plane Field Inhomogeneity, *ISBI 2007. 4th IEEE International Symposium on 12-15*, 2007 April; p.920 - 923 E.

[16] B. P. Sutton, Physics Based Iterative Reconstruction for MRI: Compensating and Estimating Field Inhomogeneity and T_2^* Relaxation. *PhD Thesis*, 2003.

[17] G. H. Glover, 3D z-shim method for reduction of susceptibility effects in BOLD fMRI. *Magn Reson Med*, 1999 Aug; 42 (2): p.290-9.

[18] H. Guo, A. W. Song, Single-shot spiral image acquisition with embedded z-shimming for susceptibility signal recovery. *J Magn Reson Imaging*, 2003 Sep; 18 (3): p.389-95.

[19] J. A. Fessler, Penalized weighted least-squares image reconstruction for positron emission tomography. *IEEE Trans Med Imag*, 1994 Jun; 13 (2): p.290-300.